The role of gravity wave drag optimization in the splitting of the Antarctic vortex in the 2002 sudden stratospheric warming

Article

Published Version

Scheffler, G., Pulido, M. and Rodas, C. (2018) The role of gravity wave drag optimization in the splitting of the Antarctic vortex in the 2002 sudden stratospheric warming. Geophysical Research Letters, 45 (13). pp. 6719-6725. ISSN 0094-8276 doi: 10.1029/2018gl077993 Available at https://centaur.reading.ac.uk/78683/

To link to this article DOI: http://dx.doi.org/10.1029/2018gl077993

Publisher: American Geophysical Union

Geophysical Research Letters

RESEARCH LETTER
10.1029/2018GL077993

Key Points:
- Gravity waves play an instrumental role in model integrations during the Antarctic SSW
- Model integrations exhibit split or displacement SSWs by changing gravity wave parameters under the same forcing at 100 hPa
- Changes of the polar vortex geometry induced by gravity wave drag contribute to resonant excitation of wave 2 activity

Correspondence to:
G. Scheffler,
guillermo.scheffler@cima.fcen.uba.ar

Citation:
Scheffler, G., Pulido, M., & Rodas, C. (2018). The role of gravity wave drag optimization in the splitting of the Antarctic vortex in the 2002 sudden stratospheric warming. *Geophysical Research Letters*, *45*, 6719–6725. https://doi.org/10.1029/2018GL077993

Received 19 MAR 2018
Accepted 9 JUN 2018
Accepted article online 19 JUN 2018
Published online 6 JUL 2018

The Role of Gravity Wave Drag Optimization in the Splitting of the Antarctic Vortex in the 2002 Sudden Stratospheric Warming

Guillermo Scheffler[1,2], Manuel Pulido[3,4,5], and Claudio Rodas[3]

[1]Centro de Investigaciones del Mar y la Atmósfera, CONICET-UBA, Buenos Aires, Argentina, [2]Department of Mathematics, FaCENA, Universidad Nacional del Nordeste, Corrientes, Argentina, [3]Department of Physics, FaCENA, Universidad Nacional del Nordeste, Corrientes, Argentina, [4]CONICET, Corrientes, Argentina, [5]Department of Meteorology, University of Reading, Reading, UK

Abstract The impact of gravity wave drag on the Antarctic sudden stratospheric warming (SSW) in 2002 is examined through a mechanistic middle atmosphere model combined with a variational data assimilation system. Significant differences in the SSW representation are found between a model integration that uses reference gravity wave parameters and one that uses parameters estimated using data assimilation. Upon identical wave forcings at 100 hPa, the vortex breakdown may arise as either a vortex splitting event or a displacement vortex event depending on gravity wave parameters. A local enhancement of Rossby waves is found in the integration with estimated parameters, leading to a split SSW. The changes in the vortex breakdown are associated with changes in the vortex geometry caused entirely by modifying the gravity wave parameters. Gravity wave drag proved to play an instrumental role in preconditioning the stratosphere near a resonant excitation point that triggers the split SSW.

Plain Language Summary Sudden stratospheric warming (SSW) events are manifestations of an abrupt change of the wintertime polar jet stream circulation, with consequences on tropospheric weather. The associated vortex breakdown is characterized by either a displacement or split of the vortex. This work focuses on the unprecedented 2002 Antarctic SSW and compares a model integration using standard model parameters, with an integration using parameters optimized using data assimilation methods. The optimized parameters are the ones in the gravity wave drag parameterization. Only the integration with optimal parameters is able to accurately reproduce the vortex splitting. Our results show that gravity wave drag parameterizations play an essential role when modeling SSWs. Data assimilation methods may be a useful tool to properly adjust these types of parameterizations.

1. Introduction

Gravity waves play a major role in the middle atmosphere of the Southern Hemisphere during wintertime. They shape the stratospheric waveguide which then influences the propagation of Rossby waves, by focusing them toward higher latitudes (Cohen et al., 2014). A manifestation of the ubiquitous interactions between gravity wave drag and Rossby wave propagation are stratospheric final warmings. Gravity waves have a significant contribution in preconditioning the polar vortex prior to final warmings in the Southern Hemisphere (Scheffler & Pulido, 2015). Most general circulation models have a pronounced delay of about 2 weeks in the representation of the stratospheric final warmings (Eyring et al., 2006; Hardiman et al., 2011). This bias is alleviated by treating some of the limitations and deficiencies in the parameterization of gravity wave drag, such as sources misspecification or lack of wave intermittency (De La Camara et al., 2016; Scheffler & Pulido, 2017).

For sudden stratospheric warming (SSW) events, the widely accepted theory suggests that the abrupt breakdown of the polar vortex can be explained in terms of transient anomalous planetary wave injections from the troposphere (Matsuno, 1971; Polvani & Waugh, 2004). However, there are some results that suggest that internal stratospheric dynamics may also play a role during SSWs. Scott and Polvani (2004) showed the existence of internal stratospheric modes that may significantly affect the propagation of upward fluxes, exerting control over the occurrence of SSWs. Recently, Birner and Albers (2017) showed that only 25% of SSWs were associated to anomalously large tropospheric wave events, while the remaining 75% of SSWs have wave fluxes that are anomalous only in the stratosphere. The role of gravity waves in SSWs is more subtle.

Matthewman and Esler (2011) identified SSWs, which are characterized by a split of the polar vortex in a quasi-geostrophic shallow-water model, as an abrupt bifurcation in the relevant parameter space which is expected to be controlled by gravity wave drag. They interpreted the split SSWs as a consequence of a self-tuned resonance excitation of Rossby waves. Albers and Birner (2014) showed that gravity wave drag is anomalously weak during vortex displacement events. On the other hand, gravity wave drag is enhanced particularly inside the vortex during vortex splitting SSW events. Therefore, gravity wave breaking may be a key element for vortex splitting SSW events, by preconditioning the vortex geometry near its resonance excitation point.

The unprecedented Antarctic SSW in September 2002 has been extensively documented (see special issue of the *Journal of Atmospheric Sciences*, 2005, Vol. 62, No. 3). This event fulfilled the World Meteorological Organization major SSW criterion (Kruger et al., 2005; McInturff, 1978) and was characterized by a splitting of the polar vortex in the middle stratosphere between 22 and 26 September (Baldwin et al., 2003). Before the event, an abnormally large upward flux of planetary wave activity reached the lower stratosphere between May and mid-September (Allen et al., 2005; Harnik et al., 2005). Manney et al. (2005) showed that for short lead time forecasts (up to 10 days before warming onset), the SSW could be reproduced as long as the 100 hPa wave amplitudes were accurately represented. Particularly, waves with wave numbers 2 and 3 played a major role for simulating the 2002 Southern Hemisphere SSW. Esler et al. (2006) showed that an unusual split vortex event like the 2002 Antarctic SSW can be explained in terms of a self-tuned resonant excitation of Rossby wave modes via the boundary forcing at specific frequencies, showing that the stratosphere can exert control on the type of SSW. Venkat Ratnam et al. (2004) found in CHAMP/GPS temperature profiles an enhancement of gravity wave activity near the edge and outside of the polar vortex 10 days prior to the SSW onset. The concomitant gravity wave drag is expected to change the mean circulation and, in turn, affect the propagation of planetary waves.

Scheffler and Pulido (2017) showed that the use of optimized parameters in a middle atmosphere model leads to an improved representation of *stratospheric final* warmings through stratospheric preconditioning. The optimized gravity wave parameters improve the complex gravity wave drag-Rossby wave interactions that take place in the Southern Hemisphere winter-summer transition. In this letter, we examine model integrations in 2002 and focus on the SSW event that occurred in the Southern Hemisphere. We use gravity wave parameters estimated with a data assimilation technique to evaluate the potential role of gravity waves during this event. Experiments, which are described in section 2, are conducted comparing the use of the spatially and temporally fixed reference gravity wave parameters, with parameters estimated using the data assimilation technique. Results (section 3) show that a proper set of gravity wave parameters is instrumental in the model integrations for shaping the vortex geometry required to support the resonance excitation that triggers the SSW event.

2. Data and Experiments

The model used in this work is the University of Reading middle atmosphere dynamical model. The model represents the fully nonlinear hydrostatic primitive equations based on potential vorticity (PV) on a hexagonal-icosahedral grid. Isentropic vertical levels range from ~100 to ~0.01 hPa. A comprehensive description of the model is given in Pulido and Thuburn (2005). Model integrations use the Montgomery potential taken from Modern-Era Retrospective Analysis for Research and Applications (MERRA) reanalyses (Global Modeling and Assimilation Office, 2011; Rienecker et al., 2011) as bottom boundary condition every 6 hr. A spectral nonorographic gravity wave drag parameterization (Scinocca, 2003) is included in the model. The dynamical model has a horizontal grid resolution of about 4° and 16 vertical levels. Because of its coarse horizontal scale, fine-scale realistic features are not represented in this model; however, the main aim in this study is to identify the main processes involved in SSW events. In particular, we focus on the interactions between the gravity wave drag parameterization and Rossby wave propagation.

The values of the gravity wave parameters are optimized using a two-step estimation method. First, an online variational data assimilation technique is used to calculate the daily zonal and meridional missing gravity wave forcing terms of the horizontal momentum equations (Pulido & Thuburn, 2005, 2006). The estimated forcing is expected to account for the momentum forcing needed by the model to give the closest evolution to MERRA reanalysis. In the second step, an offline Monte Carlo algorithm is used to estimate the parameters, as described in Pulido et al. (2012). Parameters are estimated with an offline implementation of the gravity wave drag parameterization, such that the obtained gravity wave drag profiles mimic the missing forcing profiles estimated with data assimilation, which are used as pseudo-observations. Optimal parameters are estimated daily and as a function of latitude. The procedure for parameter estimation follows the same configuration as in Scheffler and Pulido (2017).

We conducted two *free model integrations*. The term free model integrations is used to distinguish them from the integrations conducted with the assimilation system, in which the model evolution is *nudged* to the observations. In one of the free integrations, the gravity wave drag parameterization uses the reference parameter settings suggested in Scinocca (2003), except for the launched gravity wave momentum flux parameter, which is increased up to the constant value obtained in Pulido et al. (2012). This experiment will be referred to as *control integration*. In the other experiment, the launched gravity wave momentum flux, characteristic wavelength, and the saturation parameters are considered to depend on time and latitude but not on longitude. The values of the parameters are specified from the resulting optimal values of the data assimilation experiment. This integration will be referred to as *integration with optimal parameters*.

In both experiments, the dynamical model is initialized on 1 January 2002 with MERRA reanalysis and integrated during 1 year. With this initial condition, the stratospheric seasonal evolution is thoroughly represented by the model including the summer-to-winter transition, that is, the winter jet formation. The two free model integrations share exactly the same initial condition and the same bottom boundary conditions at a potential temperature of 414 K corresponding to ∼100 hPa. Therefore, differences in the winter vortex evolution between the integrations can be completely ascribed to the differences in gravity wave drag.

3. Results

The abnormal split of the polar vortex in the Southern Hemisphere during 2002 is shown in Figure 1 through PV derived from MERRA reanalyses at 10 hPa (∼900 K). On 20 September, the polar vortex is found displaced from the pole toward South America (Figure 1a). During these days, it undergoes a strong reduction of its strength. On 22 September, the polar vortex is elongated and two main centers are already apparent (Figure 1b). By 25 September, the vortex is completely split into two separated vortices at 10 hPa (Figure 1c). During the following days, the two vortices are advected and elongated (Figure 1d).

A coarse manifestation of a displacement SSW is found in the free model integration using reference gravity wave parameters (Figures 2a–2d). It achieves the required criteria to be considered a major stratospheric warming, that is, wind reversal at 10 hPa and 60°S and temperature gradient reversal between the poles and 60°S (see Charlton & Polvani, 2007; McInturff, 1978). However, the wind reversal in the control integration at 10 hPa lasts only for 2 days, while it persists for a week in MERRA. The main warming occurs with a delay of 2–3 days with respect to MERRA reanalysis. The ability to successfully predict the SSW in a 1-year model integration is attributed to the use of realistic tropospheric planetary wave forcing, incorporated through the bottom boundary of the model. The strength of the large-scale tropospheric events in 2002 leads to better SSW predictability skills in the model when compared with stratospheric final warmings.

Although the signature of the SSW is found in the control integration, the vortex structure during the breakdown process reveals several differences with respect to MERRA. It shows a weaker than observed polar winter jet. PV peaks in the control integration are about 35% weaker than in MERRA reanalysis in the week previous to the major warming (Figure 2a). The vortex at 10 hPa shows a rapid weakening between 21 and 26 September (Figures 2a and 2b). The SSW event manifests mainly as a vortex displacement SSW, even when some traces of a small amplitude wave 2 are present on 27 and 30 September (Figures 2c and 2d).

The stratospheric winter circulation in the model integration with optimal parameters is significantly modified with respect to the control integration. Figures 2e–2h depict the evolution of the polar vortex for this integration during the SSW event. In the last days prior to the sudden warming, PV meridional gradients are considerably larger than in the control integration (Figure 2e). The vortex split is clearly found in this simulation on 25 September (Figure 2f). The strength of the two vortices is remarkably close to the one found in MERRA reanalysis (Figure 1). The split occurs with a delay of 2–3 days. In the following days, the two vortices rapidly weaken (Figures 2g and 2h).

The estimated launched gravity wave momentum flux using data assimilation averaged in high latitudes (50°–80°) as a function of time is shown in Figure 3a. The parameters are smoothed using a 15-day moving average to reduce daily variability. The launched gravity wave momentum flux shows temporal variations,

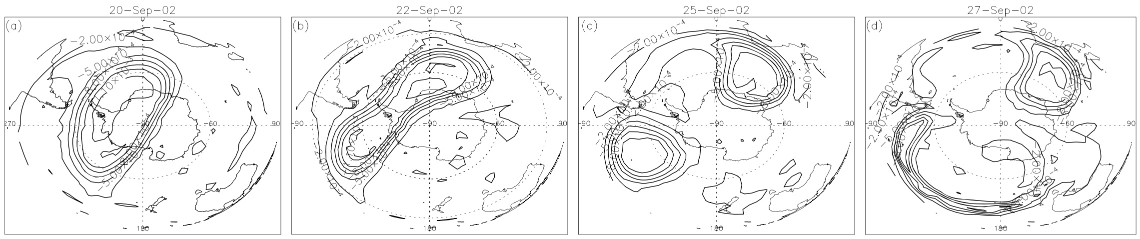

Figure 1. Potential vorticity at 10 hPa (~1,660 K) in the Southern Hemisphere for the year 2002 derived from MERRA reanalysis on (a) 20 September, (b) 22 September, (c) 25 September, and (d) 27 September. Contours at 1.5×10^{-4} km^2·kg^{-1}·s^{-1}. MERRA = Modern-Era Retrospective Analysis for Research and Applications.

reaching maximum values during winter, followed by an abrupt reduction prior to the SSW onset. Estimated parameter values suggest an increase of the launched gravity wave momentum flux during winter by more than twice the reference value. The estimated values however are strongly reduced the last 20 days before the SSW onset. This suggests that gravity wave drag has no direct role in the vortex breakdown but during the preconditioning period. The estimated E^* parameter exhibits pronounced latitudinal dependencies (see Figure 3b), characterized by increased gravity wave fluxes around 60°S during winter and up to 2 weeks prior to the SSW onset. In low latitudes, the estimated gravity wave fluxes are in general smaller than the reference value. A shift toward lower latitudes of the secondary peak is found. During this period, gravity wave drag exerted by the parameterization in the integration with optimal parameters is smaller than the one given by the reference parameters in the control integration, except near to the pole.

The indirect impact of gravity wave drag on the Rossby wave propagation and breaking is shown in Figure 4. In the control integration, Eliassen-Palm flux divergence (EPFD) at 60°S (Figure 4b) shows a single burst of planetary wave forcing distributed during late August and September. The largest peak of EPFD due to planetary wave breaking is found during the week prior to the SSW event at 10 hPa. Overall, the EPFD is around 40% weaker than in MERRA reanalysis (Figure 4a). In contrast, the EPFD from the integration with optimal parameters shows intense planetary wave breaking at high latitudes during the whole winter. Strong wave forcing events are identifiable in the month prior to the warming onset, with an intensity of up to 26 m·s^{-1}·day^{-1} above 1 hPa. The temporal distribution of EPFD in this integration is largely similar to the one derived from MERRA reanalysis. Although the forcing by gravity waves is significantly weaker than the forcing exerted by Rossby waves, it has a crucial role in conditioning the propagation and breaking of the planetary waves.

The zonal mean zonal wind averaged between 20 and 10 days before the SSW onset is shown in Figure 5. Both free model integrations show a funnel-shaped vortex and a poleward displaced winter jet with respect to the observed climatology. A wider winter jet geometry is found in the control integration, and the jet core remains

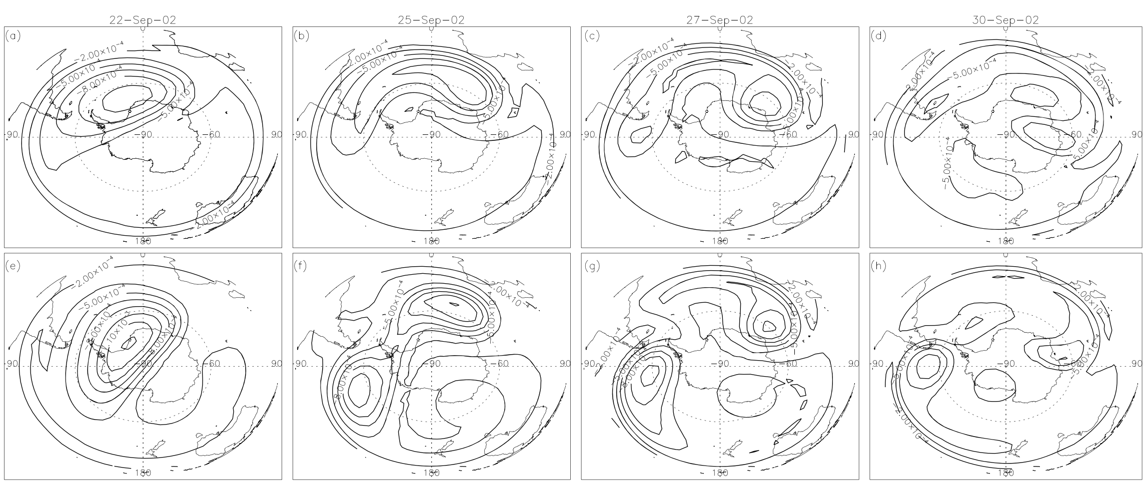

Figure 2. Potential vorticity at 10 hPa (~1,660 K) in the Southern Hemisphere for the year 2002 from the free model integrations. Upper panels show the control integration on (a) 22 September, (b) 25 September, (c) 27 September, and (d) 30 September. (e)–(h) Potential vorticity on the same dates for the integration with optimal parameters. Contours at 1.5×10^{-4}km^2·kg^{-1}·s^{-1}.

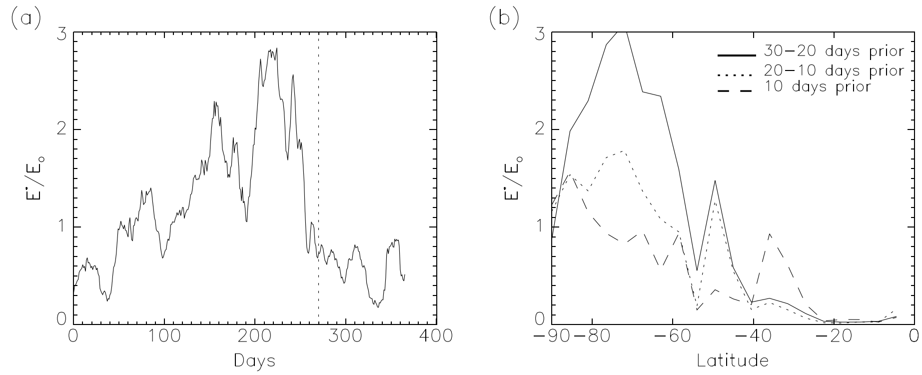

Figure 3. Launched gravity wave momentum flux, E^*, (a) estimated values as a function of time averaged between 50°S and 80°S. (b) Values as a function of latitude averaged during the 10 days prior to the sudden stratospheric warming onset (dashed line), between 10 and 20 days (dotted line), and between 20 and 30 days (solid line). Vertical dotted line corresponds to the sudden stratospheric warming onset. Values normalized with respect to its reference value $E_0 = 10 \times 2.5\sqrt{2} \cdot 10^{-4}$ Pa.

in the upper stratosphere for a larger period in this integration. In contrast, the geometry of the winter jet in the integration with optimal parameters holds a large similarity with MERRA reanalysis due to the contribution of vertical and meridionally localized gravity wave drag at middle and high latitudes and its concomitant processes. Particularly, between 40 and 2 hPa, the vertical alignment of the jet core closely resembles the winter jet on MERRA (Figure 5c). This vertical alignment of the jet during the preconditioning phase is in accordance with the characterization of a split SSW given by Albers and Birner (2014). The lower and narrower jet core in the integration with optimal parameters is also notable (Figure 5c). This is attributed to an enhanced Rossby wave propagation and breaking due to a vortex preconditioning, obtained through the optimized gravity wave drag.

While both integrations differ only in the gravity wave parameters, the optimal parameters are *zonal mean* parameters so that the parameterization cannot *directly* produce a wave 2 forcing. A mechanism that can explain the improvement in the representation of the vortex breakdown is related to wave focusing toward the pole (McIntyre, 1982). In this sense, the optimal parameter integration has the zero-wind line at higher latitudes (Figure 5c), which provides an enhancement of Rossby wave propagation toward higher latitudes and enhanced Rossby wave breaking there (see Figure 4). The latitudinal dependencies of the gravity wave flux parameter in the optimal parameter integration appears to be one of the responsible factors for shaping the waveguide toward higher latitudes. We remark that the changes found in the mean zonal wind (Figure 5) are not a direct consequence of the changes in the parameters, but they are the result of interactions between gravity wave drag and planetary waves during the preconditioning phase.

Two aspects produced by the optimal parameters appear to contribute to the triggering of a self-tuned resonance excitation. Gravity wave drag is known to be mainly responsible for the closing of the jets in the mesosphere (Pulido & Thuburn, 2008). This effect is apparently contributing to the descent of the jet core

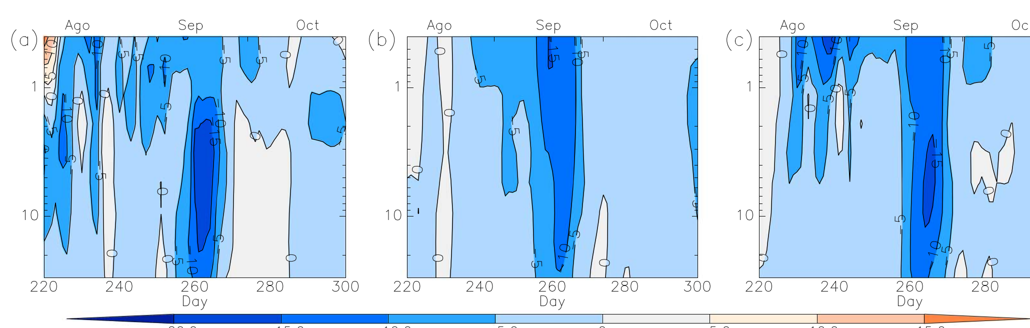

Figure 4. Eliassen-Palm flux divergence at 60°S as a function of time. (a) MERRA, (b) control integration, and (c) integration with optimal parameters. Day 268 corresponds to the SSW onset on MERRA reanalysis. Data have been smoothed using a moving 5-day time average window. Contours are at 5 m·s^{-1}·day^{-1}.

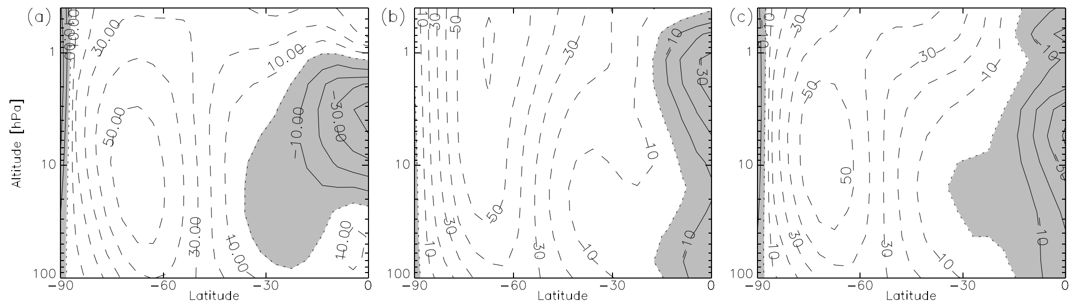

Figure 5. Zonal mean wind averaged between 20 and 10 days before the sudden stratospheric warming. (a) MERRA, (b) control integration, and (c) integration with optimal parameters. Contours at 10 $m \cdot s^{-1} \cdot day^{-1}$. Negative values are shaded. MERRA = Modern-Era Retrospective Analysis for Research and Applications.

in the optimal parameter integration (Figure 5). The concomitant negative shear in the upper stratosphere above the jet core contributes to making the waves evanescent, not allowing them to propagate upward, and therefore facilitating the resonance mechanism. A second characteristic is the shift in the zero-wind line toward higher latitudes. Apart from focusing planetary waves, this produces a reduction in the zonal mean wind threshold required for the resonance (Plumb, 1981).

4. Conclusions

In this letter, the representation of the 2002 Antarctic SSW in a middle atmosphere model is examined. Whereas the model used in this work has a coarse resolution, it is able to give some of the most salient features of the 2002 SSW. The model is based on PV in an icosaedral-hexagonal grid which is particularly suited to capture adequately planetary wave mean flow interactions as well as gravity wave drag effects on the stratosphere dynamics (Pulido, 2014).

We compare a free model integration that uses the standard configuration of a nonorographic gravity wave drag parameterization with an integration using optimal gravity wave drag parameters estimated with a data assimilation technique. The use of optimal parameters improves significantly the representation of the SSW event. The temporal and latitudinal variability of gravity wave parameters improves the representation of gravity wave drag-Rossby wave interactions which lead to a more realistic zonal mean circulation. The changes to the mean flow produced by these interactions include the narrowing and poleward shifting of the planetary waveguide and the lowering of the jet core with an intensification of zonal mean zonal wind in the lower stratosphere. These changes give support to the triggering of a self-tuned resonance that leads to the vortex split.

Since the optimized parameters in the experiments do not have longitudinal variations, the enhancement of wave 2 activity in the polar region cannot be attributed directly to gravity wave forcing. Furthermore, a decrease in the gravity wave flux is estimated before the onset of the SSW; this suggests that in our experiments the SSW onset cannot be attributed to a noise-induced transition as in Birner and Williams (2008). In this work, the SSW is established in both experiments. The forcing through gravity waves proved to be an indirect, albeit crucial, instrument for modeling the type of vortex breakdown.

We have found evidence that given the same boundary forcing, the stratosphere may manifest both types of SSWs: either a displacement SSW, dominated by waves with wave number 1, or a split SSW mostly affected by waves with wave number 2. The only difference between these two manifestations of SSWs was the geometry of the Antarctic vortex (see also De La Camara et al., 2017). We show that, in the experiments, gravity wave activity is responsible for the bifurcation between displacement and split vortex events. This is in agreement with Matthewman and Esler (2011) and Albers and Birner (2014). Matthewman and Esler (2011) use a surf zone PV parameter which in reality may indeed be partially controlled by gravity wave drag.

Finally, the existence of Rossby waves triggered by barotropic instabilities (see Rodas & Pulido, 2017) was found in the experiments, but it is not explored in this work. A follow-up work is underway to quantify the relative role of these instabilities in the triggering of SSWs.

Acknowledgments
This work used the computational facilities at CECONEA (UNNE) and was partially funded by ANPCyT PICT2015-2368. MERRA data have been provided by the Global Modeling and Assimilation (GMA) at NASA Goddard Space Flight Center and is available through the NASA GES-DISC archive.

References

Albers, J. R., & Birner, T. (2014). Vortex preconditioning due to planetary and gravity waves prior to sudden stratospheric warmings. *Journal of the Atmospheric Sciences*, *71*, 4028–4054.

Allen, D. R., Coy, L., Eckermann, S. D., Manney, G. L., Hogan, T. F., & Kim, Y.-J. (2005). NOGAPS-ALPHA simulations of the 2002 Southern Hemisphere stratospheric major warming. *Monthly Weather Review*, *134*, 498–518.

Baldwin, M., Hirooka, T., O'Neill, A., Yoden, S., Charlton, A. J., Hio, Y., & Yoden, S. (2003). Major stratospheric warming in the Southern Hemisphere in 2002: Dynamical aspects of the ozone hole split. *SPARC Newsletter*, *20*, 24–26.

Birner, T., & Albers, J. R. (2017). Sudden stratospheric warmings and anomalous upward wave activity flux. *SOLA*, *13*, 8–12.

Birner, T., & Williams, P. D. (2008). Sudden stratospheric warmings as noise-induced transitions. *Journal of the Atmospheric Sciences*, *65*, 3337–3343.

Charlton, A. J., & Polvani, L. M. (2007). A new look at stratospheric sudden warmings. Part I: Climatology and modeling benchmarks. (2007). *Journal of Climate*, *20*, 449–470.

Cohen, N. Y., Gerber, E. P., & Bühler, O. (2014). What drives the Brewer–Dobson circulation? *Journal of the Atmospheric Sciences*, *71*, 3837–3855.

De La Camara, A., Albers, J. R., Birner, T., Garcia, R. R., Hitchcock, P., Kinnison, D. E., & Smith, A. K. (2017). Sensitivity of sudden stratospheric warmings to previous stratospheric conditions. *Journal of the Atmospheric Sciences*, *74*, 2857–2877.

De La Camara, A., Lott, F., & Abalos, M. (2016). Climatology of the middle atmosphere in LMDz: Impact of source-related parameterizations of gravity wave drag. *Journal of Advances in Modeling Earth Systems*, *8*, 1507–1525. https://doi.org/10.1002/2016MS000753

Esler, J. G., Polvani, L. M., & Scott, R. K. (2006). The Antarctic stratospheric sudden warming of 2002: A self-tuned resonance?*Geophysical Research Letters*, *33*, L12804. https://doi.org/10.1029/2006GL026034

Eyring, V., Butchart, N., Waugh, D. W., Akiyoshi, H., Austin, J., Bekki, S., et al. (2006). Assessment of temperature, trace species, and ozone in chemistry-climate model simulations of the recent past. *Journal of Geophysical Research*, *111*, D22308. https://doi.org/10.1029/2006JD007327

Global Modeling and Assimilation Office (2011). MERRA 3D analyzed state, meteorology instantaneous 6-hourly, version 5.2.0, Greenbelt, MD, USA. Accessed May 2013 at https://doi.org/10.5067/ADAWH64DCRU0

Hardiman, S. C., Butchart, N., Charlton, A. J., Shaw, T., Akiyoshi, H., et al. (2011). Improved predictability of the troposphere using stratospheric final warmings. *Journal of Geophysical Research*, *116*, D18113. https://doi.org/10.1029/2011JD015914

Harnik, N., Scott, R. K., & Perlwitz, J. (2005). Wave reflection and focusing prior to the major stratospheric warming of September 2002. *Journal of the Atmospheric Sciences*, *62*, 640–650.

Kruger, K., Naujokat, B., & Labitzke, K. (2005). The unusual midwinter warming in the Southern Hemisphere stratosphere 2002: A comparison to Northern Hemisphere phenomena. *Journal of the Atmospheric Sciences*, *62*, 603–613.

Manney, G. L., Sabutis, J. L., Allen, D. R., Lahoz, W. A., Scaife, A. A., & Randall, C. E. (2005). Simulations of dynamics and transport during the September 2002 Antarctic major warming. *Journal of the Atmospheric Sciences*, *62*, 690–707.

Matsuno, T. (1971). A dynamical model of the stratospheric sudden warming. *Journal of the Atmospheric Sciences*, *28*, 1479–1494.

Matthewman, N. J., & Esler, J. G. (2011). Stratospheric sudden warmings as self-tuning resonances. Part I: Vortex splitting events. *Journal of the Atmospheric Sciences*, *68*, 2481–2504.

McInturff, R. M. (1978). Stratospheric warmings: Synoptic, dynamic and general circulation aspects. *NASA Reference Publ*. NASA-RP-1017, (174 pp.).

McIntyre, M. (1982). How well do we understand the dynamics of stratospheric warmings?*Journal of the Meteorological Society of Japan*, *60*, 37–65.

Plumb, R. (1981). Instability of the distorted polar night vortex: A theory of stratospheric warmings. *Journal of the Atmospheric Sciences*, *38*, 2514–2531.

Polvani, L. M., & Waugh, D. W. (2004). Upward wave activity flux as a precursor to extreme stratospheric events and subsequent anomalous surface weather regimes. *Journal of Climate*, *17*, 3548–3554.

Pulido, M. (2014). A simple technique to infer the missing gravity wave drag in the middle atmosphere using a general circulation model: Potential vorticity budget. *Journal of the Atmospheric Sciences*, *71*, 683–696.

Pulido, M., Polavarapu, S., Shepherd, T. G., & Thuburn, J. (2012). Estimation of optimal gravity wave parameters for climate models using data assimilation. *Quarterly Journal of the Royal Meteorological Society*, *138*, 298–309.

Pulido, M., & Thuburn, J. (2005). Gravity-wave drag estimation from global analyses using variational data assimilation principles. I: Theory and implementation. *Quarterly Journal of the Royal Meteorological Society*, *131*, 1821–1840.

Pulido, M., & Thuburn, J. (2006). Gravity-wave drag estimation from global analyses using variational data assimilation principles. II: Case study. *Quarterly Journal of the Royal Meteorological Society*, *132*, 1527–1543.

Pulido, M., & Thuburn, J. (2008). The seasonal cycle of gravity wave drag in the middle atmosphere. *Journal of Climate*, *21*, 4664–4679.

Rienecker, M. M., Suarez, M. J., Gelaro, R., Todling, R., Bacmeister, J., Liu, E., et al. (2011). MERRA: NASA's Modern-Era Retrospective Analysis for Research and Applications. *Journal of Climate*, *24*, 3624–3648.

Rodas, C., & Pulido, M. (2017). A climatology of Rossby wave generation in the middle atmosphere of the Southern Hemisphere from MERRA reanalysis. *Journal of Geophysical Research: Atmospheres*, *122*, 8982–8997. https://doi.org/10.1002/2017JD026597

Scheffler, G., & Pulido, M. (2015). Compensation between resolved and unresolved wave drag in the stratospheric final warmings of the Southern Hemisphere. *Journal of the Atmospheric Sciences*, *72*, 4393–4411.

Scheffler, G., & Pulido, M. (2017). Estimation of gravity-wave parameters to alleviate the delay in the Antarctic vortex breakup in general circulation models. *Quarterly Journal of the Royal Meteorological Society*, *143*, 2157–2167.

Scinocca, J. F. (2003). An accurate spectral nonorographic gravity wave drag parameterization for general circulation models. *Journal of the Atmospheric Sciences*, *60*, 667–682.

Scott, R. K., & Polvani, L. M. (2004). Stratospheric control of upward wave flux near the tropopause. *Geophysical Research Letters*, *31*, L02115. https://doi.org/10.1029/2003GL017965

Venkat Ratnam, M., Tsuda, T., Jacobi, C., & Aoyama, Y. (2004). Enhancement of gravity wave activity observed during a major Southern Hemisphere stratospheric warming by CHAMP/GPS measurements. *Geophysical Research Letters*, *31*, L16101. https://doi.org/10.1029/2004GL019789